Project Report
2006-2007

Title:

Center for Applications of Single-Walled Carbon Nanotubes

PI: Daniel E. Resasco
Award Register#: ER64239 0012293

Project ID:
0012293

Program Manager:
Marvin Stodolsky
Phone: 301-903-4475
Division: SC-23.2

Abstract:

This report describes the activities conducted under a Congressional Direction project whose goal was to develop applications for Single-walled carbon nanotubes, under the Carbon Nanotube Technology Center (CANTEC), a multi-investigator program that capitalizes on OU's advantageous position of having available high quality carbon nanotubes. During the first phase of CANTEC, 11 faculty members and their students from the College of Engineering developed applications for carbon nanotubes by applying their expertise in a number of areas: Catalysis, Reaction Engineering, Nanotube synthesis, Surfactants, Colloid Chemistry, Polymer Chemistry, Spectroscopy, Tissue Engineering, Biosensors, Biochemical Engineering, Cell Biology, Thermal Transport, Composite Materials, Protein synthesis and purification, Molecular Modeling, Computational Simulations.

In particular, during this phase, the different research groups involved in CANTEC made advances in the tailoring of Single-Walled Carbon Nanotubes (SWNT) of controlled diameter and chirality by Modifying Reaction Conditions and the Nature of the catalyst; developed kinetic models that quantitatively describe the SWNT growth, created vertically oriented forests of SWNT by varying the density of metal nanoparticles catalyst particles, and developed novel nanostructured SWNT towers that exhibit superhydrophobic behavior. They also developed molecular simulations of the growth of Metal Nanoparticles on the surface of SWNT, which may have applications in the field of fuell cells.

In the area of biomedical applications, CANTEC researchers fabricated SWNT Biosensors by a novel electrostatic layer-by-layer (LBL) deposition method, which may have an impact in the control of diabetes. They also functionalized SWNT with proteins that retained the protein's biological activity and also retained the near-infrared light absorbance, which finds applications in the treatment of cancer.

At the same time, they investigated methods for synthesizing composites of SWNT and polymers and characterized their electrical and mechanical behavior. They also produced aluminum/nanotube composites using aqueous dispersion of SWNT.

Project Report (2006-2007)

CARBON NANOTUBES TECHNOLOGY CENTER (CANTEC)

This report describes the activities conducted under a Congressional Direction project whose goal was to develop applications for Single-walled carbon nanotubes, under the Carbon Nanotube Technology Center (CANTEC). Eleven faculty members and their students from the College of Engineering participated actively (Resasco, Harwell, Schmidtke, Grady, McFetridge, Harrison, Striolo, Saha, Altan, Renaker, and Olson). The expertise of this multidisciplinary group covers a number of areas: Catalysis, Reaction Engineering, Nanotube synthesis, Surfactants, Colloid Chemistry, Polymer Chemistry, Spectroscopy, Tissue Engineering, Biosensors, Biochemical Engineering, Cell Biology, Thermal Transport, Composite Materials, Protein synthesis and purification, Molecular Modeling, Computational Simulations

Research Projects:
• Controlled synthesis, purification,
• SWNT-surfactant-surfaces interactions
• Metal-SWNT composites
• Polymer-SWNT composites
• SWNT based biosensors
• Cell-nanotube interactions
• Nanotube-neural interface

Since the program started in June 2006, the group has made more than 10 oral presentations, it has submitted 13 articles for publication and it has submitted or is in the process to submit 9 grants to various funding agencies including NSF, DOE, NIH, and the state agency OCAST.

Company associated to CANTEC: SouthWest NanoTechnologies, Inc. (SWeNT) is an Oklahoma corporation that was founded in April 2001 to make single wall carbon nanotubes a commercial reality. SWeNT has an exclusive license from the University of Oklahoma to make and sell carbon nanotubes using the patented CoMoCAT® process, which gives it a distinct competitive advantage in the areas of quality control and process scalability.

Students supported by the program:

- Naveen Palwai, Ph.D. student **(graduated 7-26-07)** – proteins/SWNT
- Giulio Lolli, PhD student **(graduated 07-20-07)** – SWNT synthesis
- Federico Scodelaro, MS student **(graduated 12-15-07)** – SWNT synthesis
- Youdan Wang, MS student **(graduated 12-15-07)** SWNT biosensors
- Luis Neves, Ph.D. student - proteins/SWNT
- B.H. Morrow, Ph.D. student – modelling SWNT
- Israel Chavez-Sumarriva, Ph.D. student – SWNT/polymer composites
- Ta-Wei Tsai, MS student, SWNT biosensors
- David Martyn, Posdoctoral student, SWNT functionalization
- Jeremy Bjorlie, mechanical engineering MS student
- Jeremiah Miller, mechanical engineering MS student
- Jason Watkins, mechanical engineering MS student

CANTEC Publications during the reported period:

- "Controlling the growth of vertically-oriented single-walled carbon nanotubes by varying the density of Co-Mo catalyst particles" Liang Zhang; Yongqiang Tan, **Daniel E. Resasco**, *Chemical Physics Letters* 422, 198-203, 2006.
- "Tailoring (n,m) structure of single-walled carbon nanotubes by modifying reaction conditions and the nature of the support of CoMo catalysts." **Giulio Lolli**, Liang Zhang, Leandro Balzano, Nataphan Sakulchaicharoen, Yongqiang Tan, and **Daniel E. Resasco**, *Journal of Physical Chemistry B*, 2006; 110(5); 2108-2115
- "A Novel Hybrid Carbon Material" Albert G. Nasibulin, Peter V. Pikhitsa, Hua Jiang, David P. Brown, Arkady V. Krasheninnikov, Anton S. Anisimov, Paula Queipo, Anna Moisala, David Gonzalez, Gunther Lientschnig, Abdou Hassanien, Sergey D. Shandakov, **Giulio Lolli, Daniel E. Resasco**, Mansoo Choi, David Tománek, and Esko I. Kauppinen, *Nature Nanotechnology* 2(3), 156-161 2007
- "Influence of a Top Crust of Entangled Nanotubes on the Structure of Vertically Aligned Forests of Single-Walled Carbon Nanotubes" L. Zhang, Z. Li, Y. Tan, **G. Lolli**, N. Sakulchaicharoen, F. G. Requejo, B. Simon Mun, and **Daniel E. Resasco**, *Chemistry of Materials* 18 (23): 5624-5629, 2006
- **Palwai NR, Martyn DE, Neves LFF**, Tan Y, **Resasco DE, Harrison RG**. Retention of biological activity and near-infrared absorbance upon adsorption of horseradish peroxidase on single-walled carbon nanotubes. *Nanotechnology* 2007;18:235601.
- **B.H. Morrow** and **A. Striolo**, *Morphology and Diffusion Mechanism of Platinum Nanoparticles Supported on Carbon Nanotube Bundles*, *Journal of Physical Chemistry* C, 111 (2007) 17905.
- **B.H. Morrow** and **A. Striolo**, Platinum Nanoparticles on Carbonaceous Materials: Effect of Support Geometry on Nanoparticle Mobility, Morphology, and Melting, *Nanotechnology*, (2008) submitted.
- **B.P. Grady**. "The Use of Solution Viscosity to Characterize Single-Walled Carbon Nanotube Dispersions", *Macromolecular Chemistry and Physics*, 207, 2167 (2006).
- F. Buffa, G.A. Abraham, **B.P. Grady and D.E. Resasco**, "Effect of Nanotube Functionalization on the Properties of Single-walled Nanotube-Polyurethane Composites" *Journal of Polymer Science: Part B Polymer Physics*, 45, 490 (2007).
- M. Ha, **B.P. Grady, D.E. Resasco**, L. Balzano, W.T. Ford, "Composites of Single-wall Carbon Nanotubes and Copolymer Latices of Styrene and Isoprene" *Macromolecular Chemistry and Physics*, 208, 446 (2007).
- M.N. Tchoul, W.T. Ford, M. L. P. Ha, **I. Chavez-Sumarriva, B. P. Grady, G. Lolli, D. E. Resasco**, and S. Arepalli, "Composites of Single-walled Carbon Nanotubes and Polystyrene: Preparation and Electrical Conductivity" submitted to *Chemistry of Materials*
- **Wang Y**, Joshi PP, Hobbs KL, Johnson MB, **Schmidtke DW**, "Nanostructured Biosensors Built by Layer-By-Layer Electrostatic Assembly of Enzyme-Coated Single-Walled Carbon Nanotubes and Redox Polymers". *Langmuir* 22:9776-9783, 2006
- Water self-diffusion through narrow oxygenated carbon nanotubes, **Striolo,** *Nanotechnology* , 18 Article Number: 475704 (2007)
- **Olson, B.W., Watkins, J., Butler, Z., Lolli, G**., "Aqueous Pre-dispersion of Carbon Nanotubes in Powdered Aluminum Composites", *Adv. Eng. Mtrls*, submitted for review. (A CaNTeC collaboration)

Patents:

- **Harrison, RG, and Resasco, DE**. Cancer Treatment Using Targeted Single-Walled Carbon Nanotubes. U.S. Provisional Patent Application 2007; 60/901/894.

A) Controlled synthesis of Single-walled carbon nanotubes

PI: Daniel Resasco

Project A.1: Synthesis of Single-Wall-Carbon-Nanotubes from methane decomposition with high selectivity.

The standard CoMoCAT method developed at the University of Oklahoma is based on the disproportionation of CO. For economic, safety, and process reasons, it is desirable to be able to obtain similar selectivities by using methane as a feedstock. Also, the nanotube diameter obtained with the standard CoMoCAT is always around 1.0 nm or less. For some applications may be desirable to produce nanotube with larger diameters. In previous investigations, it has been observed that methane decomposition results in nanotubes of diameters larger than 2 nm (1-2). Unfortunately, to date, no catalyst has been able to obtain with CH_4 feed comparable selectivities to SWNT as it is obtained on Co-Mo/SiO_2 with CO. In this project, we have investigated methane as a feed on MgO-supported catalysts with Co-Mo active species at varying loadings and Co/Mo ratios.

The catalysts used have the general composition $Co_xMo_yMg_{1-x-y}O$ and were prepared by thermal decomposition (combustion) of the precursor salts, using citric acid as the fuel. In our standard catalyst, x=0.0075 and y=0.0025, resulting in a total metal content of 1 at.% and a Cobalt/Molybdenum ratio of 3:1. Experiments were also performed varying the Co/Mo ratio. In those cases, the Co content is kept constant at 1.1 wt%, as in the standard catalyst. The metal precursors used for the preparation are $Mg(NO_3)_2.9H_2O$, $Co(NO_3)_2.6H_2O$ and $(NH_4)_6Mo_7O_{24}.4H_2O$. The salts are dissolved in water (used in small amounts) along with citric acid (used as the fuel) and the solution is quickly evaporated and calcined in a furnace at 500 ºC. The resulting material is then ground into a fine powder for use. To study the effect of the composition of the support, samples with an aluminum-doped magnesium oxide support were prepared. The Mg/Al ratio was set to 3:1 and the preparation only differed in that the additional precursor salt ($Al(NO_3)_3.9H_2O$) was added to the solution to be calcined.

XPS data was recorded on a Physical Electronics PHI 5800 ESCA System with monochromatic AlKα X rays (1486.6 eV) operated at 350 W and 15 kV. XRD patterns were acquired using a Bruker AXS Discovery G8 equipped with a GADDS aerial detector. In a typical experiment the acquisition time was about 12 hours. The resulting diffractograms were analyzed using a powder diffraction database PDF-2 2004 from ICDD.

Nanotube growth tests were performed in a vertically oriented fixed-bed reactor configuration, consisting of a tube furnace, temperature controller and gas mass-flow controllers. The reactor is a quartz tube of 10 mm inner diameter. In a typical activity test, around 200 mg of catalyst are placed inside a quartz tube (½ inch outside diameter), and are reduced at 500 ºC for 30 minutes and then heated to reaction temperature in a He atmosphere. The flow rates used were 180 std cm^3 min^{-1}. After the growth of SWNT has proceeded (typical reaction times are around 30 minutes) the furnace is turned off and the quartz reactor is cooled down to room temperature by purging it in a He atmosphere.

Liquid-phase purification protocols were performed using water, mild acid solutions (typically, HCl) and reflux conditions in stronger acids (HNO_3/H_2SO_4), coupled with sonication, and followed by vacuum filtering and washing with excess deionized water. The feasibility of gas-phase treatments for enhancing the quality of nanotube samples was studied by using a low temperature oxidation.

Raman spectroscopy of both spent catalyst and purified SWNT was performed in a Jovin Yvon-Horiba LabRam 800 equipped with an air-cooled CCD detector and a He–Ne laser (632.8 nm).

The temperature-programmed oxidation (TPO) of a sample can help in the quantification of the different forms of carbon available on it. SWNTs are oxidized in a narrow temperature range, which is above the oxidation of amorphous carbon and below the oxidation of both graphitized carbon and MWNT (9). Temperature Programmed Oxidation was performed by flowing 5% O_2/He over about 15 mg of spent catalyst sample while heating it at a linear rate of 10ºC/min. The CO_2 resulting from the oxidation of SWNT is converted to CH_4 on a methanator reactor and the methane signal is monitored on a Flame Ionization Reactor, SRI model 110 FID. TEM images were obtained in a JEOL JEM-2000FX transmission electron microscope. The nanotube samples (both raw and purified) were dispersed in 2-propanol and ultrasonicated for 30 minutes. A few drops of this dispersion were deposited and let dry on a TEM grid.

Main results

1 Effect of the Catalyst Composition

1.1 Effect of Co/Mo ratio: The effect of the catalyst composition on its performance to yield high quality carbon nanotubes was investigated by preparing catalysts of different compositions, but with equivalent total cobalt weight loading (i.e. the effect of addition of molybdenum was studied). Molybdenum fractions were varied from 0 (only cobalt as active metal) to 0.5 (same number of moles of cobalt as those of molybdenum). Activity tests were conducted during 30 minutes on a CH_4 (18%) / H_2 mixture. The Raman spectra of the as-produced samples are shown in Figure 1. In all four cases the typical characteristic vibration modes corresponding to carbon nanotubes appear namely radial breathing mode, G band and D band. The *quality factor* was defined as:

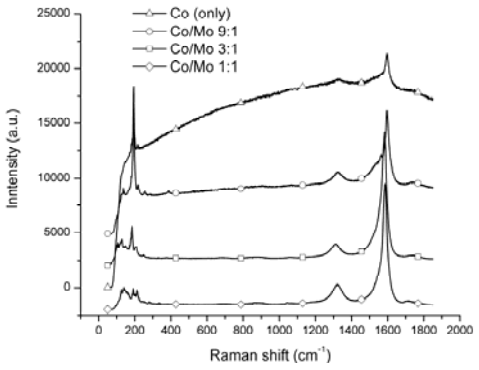

Figure 1. Raman spectra of as-produced samples from catalysts with varying Co/Mo ratios

$$Q_F = 1 - \frac{I_D}{I_G}$$

The values calculated from the spectra are:

- Co-only=0.84
- Co/Mo:9/1=0.87
- Co/Mo:3/1=0.92
- Co/Mo:1/1=0.95

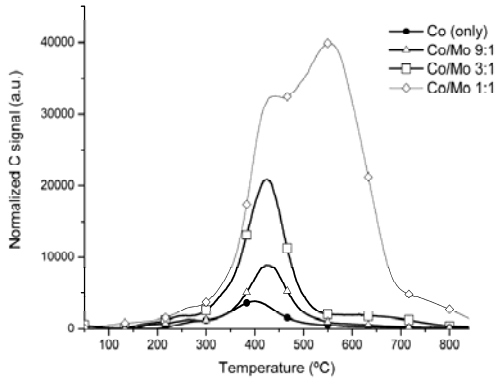

Figure 2. TPO profiles for as-produced samples from catalysts with varying Co/Mo ratio

On the other hand, the calculated yields from the TPO profiles shown in Fig. 2 are: 1.5% (Co-only), 2.6% (Co / Mo : 9 / 1), 5.2% (Co / Mo : 3 / 1) and 21.6% (Co / Mo : 1/1). There is a monotonic increase in total carbon yield with Mo content, in part attributable to increase in metal loading of the catalyst, but also other effects might be playing a role which will be investigated in more detail.

1.2 Effect of Metal Loading: To study the effect of metal loading on the catalyst, samples with 1, 2 and 3 atomic percent metals (1.7, 3.3 and 4.9 wt %) were prepared and tested in the regular conditions. The Raman spectra are shown in Figure 4. The Raman spectra show all the typical bands corresponding to carbon nanotubes.

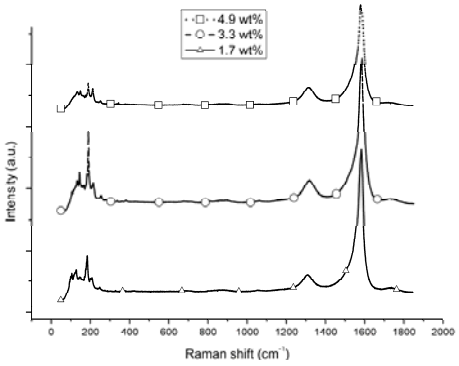

Figure 3. Raman spectra of as-produced samples obtained with different catalyst metal loadings.

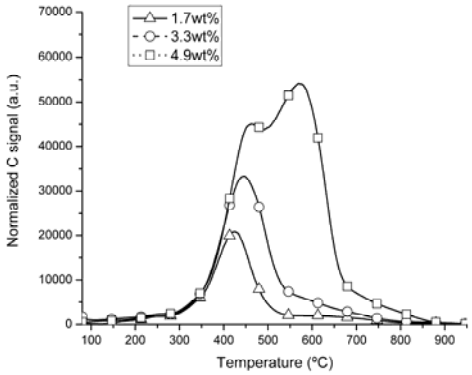

Figure 4. TPO results of as-produced carbon nanotube samples prepared with different catalyst metal loadings.

The sample with 1.7 wt% metal loading shows a relatively strong radial breathing mode and a lower I_D/I_G ratio, as evidenced in the quality factor values. The values of the quality factors are: 0.92 (1.7%wt), 0.88 (3.3%wt) and 0.86 (4.9%wt), respectively. The

types of carbon species present in the sample were investigated using TPO. The oxidation profiles for each of these samples are presented in Figure 4. The carbon yields increase with increasing metal content, but for the highest loading sample, two different types of materials show in the TPO profile (one centered at around 440ºC, and the other one at 570ºC).

The catalyst with 3.3 wt% total metal loading strikes as the most suitable for a scale-up, given that it produces the highest quality nanotubes of the set, with an very good carbon yield of over 12%.

1.3 Effect of the Catalyst Pellet Size: The use of pellets instead of fine powder catalysts makes sense in an industrial context, where fluidized beds are used as reactors and catalyst entrapment has to be controlled. For this reason, three different pellet size ranges were studied: 450-825 μm pellets, 75-150 μm pellets, and a below-75 μm particle size (considered as fine powder). The highest quality product is obtained from the sub-75 μm powder (results not shown). In the other cases, especially for the large pellets, a high degree of heterogeneity was observed, with a low average for the quality factor (below 0.70). The fine powder also has the highest activity. Selectivity towards carbon nanotubes vs. other forms of carbon decreases dramatically for the larger pellets.

1.4 Effect of the Catalyst Reduction Conditions: Several catalyst reduction conditions were studied in order to find an optimum for carbon nanotube production. Initially, four different situations were analyzed: 1) no pre-reduction of the catalyst, 2) pre-reduction at the reaction temperature, that is, 900°C, 3) reduction at 400°C and 4) reduction at 500°C. The quality factors (results not shown) for the sample reduced at 900°C and the sample with no pre-reduction are below 0.75. The other two samples are of better quality, especially the one pre-reduced at 500°C, which appears to be the optimum. It is of industrial interest the possibility to separate the reduction and reaction processes, rather than do them both in the same reaction batch (in-situ). In that way, for example, a catalyst vendor could provide a pre-reduced catalyst which is ready for production.

In order to evaluate this possibility, we performed a passivation experiment where a catalyst sample was reduced at 500°C, cooled down to room temperature and exposed to air. One reaction was run after doing this, while another reaction was run after storing the pre-reduced catalyst for 48 hours at room temperature in non-inert atmosphere. The experiments showed that the offline pre-reduction does not work for this catalyst system, as evidenced by the considerably lower quality of the resulting product, even when running a reaction right after the catalyst was pre-reduced and cooled down. Another possibility that was analyzed was to perform a linear heating ramp under hydrogen rather than ramping to 500°C in hydrogen and keeping the temperature constant at 500°C for 30 minutes during the reaction. This was also studied because it might ease design specifications in the industrial scale-up of the process. Two reaction ramps were considered: 1) a linear ramp to 550°C under hydrogen, and 2) a linear ramp in hydrogen up to the reaction temperature (900°C). Again, the product pre-reduced with a linear ramp up to 900°C shows a poor performance, but the sample pre-reduced by heating up to 550°C in hydrogen shows a similar performance to our standard material, with a quality factor of 0.86, just a few percent points below the standard. If during the potential scale-up of the process this linear increase in temperature during the reduction was easier to implement than the stationary reaction at 500°C, the end temperature of the heating ramp could be tuned to find an optimum value. For our purposes, at the laboratory scale we will choose 500°C reduction for 30

minutes (with prior ramp to 500°C) under pure hydrogen as the optimal point.

2 Effect of Reaction Operating Conditions

2.1 Effect of Time on Stream: The effect of reaction time on the quality of as-produced samples was analyzed by running our standard catalyst for varying times in the regular conditions (reduction in H_2 at 500°C for 30 minutes, and reaction at 900°C in 18% CH_4 in H_2 mixture). The optimum reaction time (results not shown) appears to be 30 minutes. Running the reaction for a longer time, results in deposition of amorphous carbon, or in increased defects in the tubes already grown.

2.2. Effect of Carbon Source Concentration: It is interesting to know more about the effect of hydrogen concentration in the reaction mixture. Four compositions of reaction mixtures were studied, while keeping the rest of the conditions constant, and results are shown in Figure 5. Of the four gas phase compositions that we tried, the 18% CH_4/H_2 yields the best results in terms of quality according to the Raman spectra. Hydrogen seems to work by promoting the reverse reaction (methane formation by reacting with deposited carbon) and it is apparently selective first to forms of carbon with more defects. The 6% sample showed a very low yield (grayish color of as-produced sample at the end of the reaction) which usually shows in the Raman spectrum like a high background signal.

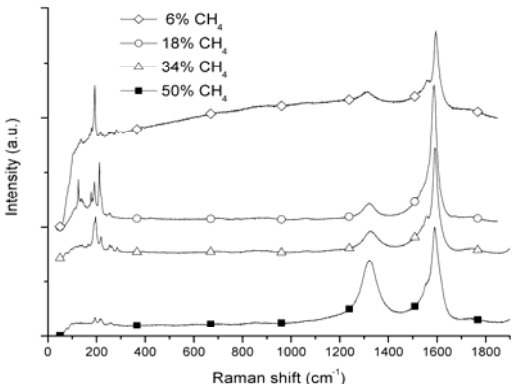

Figure 5. Raman spectra of as-produced samples obtained by changing the methane concentration in the reaction mixture.

2.3. Effect of Reaction Temperature: We studied the effect of reaction temperature on the quality of the as-produced material as measured by the I_D/I_G intensity in the Raman spectra. Three reaction temperatures were tried, while keeping the reaction time at 30 minutes using 18% CH_4 in hydrogen, and leaving the reduction conditions unchanged (30 minutes in H_2 at 500°C). The best conditions appear to be when the reaction runs at 900°C, and probably raising the temperature is better than lowering it. This could also be observed in the yield. Even at first glance, the yield for the sample produced at 850°C was considerably lower than in the other two cases, judging by the grayish color of the product. It can also be observed in the relatively noisy Raman signal, where all spectra were acquired using the same energy flux, indicating a lower number of counts per unit time due to less material present.

3. Purification results.

To purify the as-produced material was dispersed in deionized water and sonicated for 30 minutes in a bath sonicator at 60°C. The pH of the resulting dispersion was about 10, due to the basic nature of the magnesium oxide used as the support. In order to increase the solubility of the magnesium oxide and move it to the liquid phase, the pH was lowered by adding a HCl solution. The dispersion was then bath sonicated again for an extra 30 minutes to allow forcomplete dissolution, and then vacuum filtered and finally washed with deionized water. The Raman spectra of the as-produced sample and the purified sample are shown in Figure 6.

We can observe that the disordered vibration mode increases greatly, probably due to the attack by the acid of the weaker nanotubes or the tubes with more defects. This is one of the reasons it is best to start with a raw material with the highest possible quality, as the nanotubes with defects will be the least resistant to the acid attack. In order to improve the quality of the purified materials was carried out a low temperature oxidation of the as-produced sample in static air. After this treatment (results not shown), the quality of the product improved noticeably due to the elimination of the amorphous fractions present in the as-produced sample. This method can be combined with the liquid phase purification in order to produce better results.

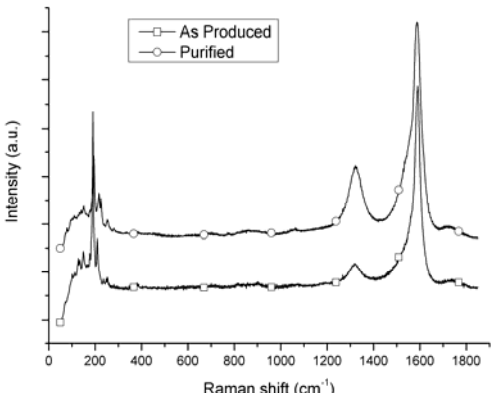

Figure 6. Raman spectra of as-produced material and purified product, using a 0.5M HCl solution.

Figures 7 and 8 show TEM and AFM micrographs of the product obtained through all this production protocol, showing good long bundles and clean individual tubes. The diameters of the nanotubes obtained with this method are larger than with methods such as CoMoCAT®, a fact which might be of interest in the potential applications of these materials.

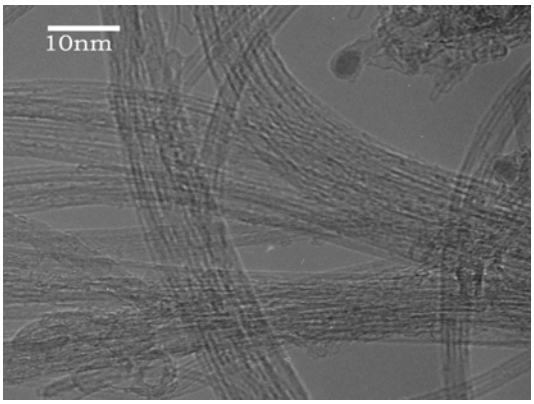

Figure 7. TEM of purified SWNT sample.

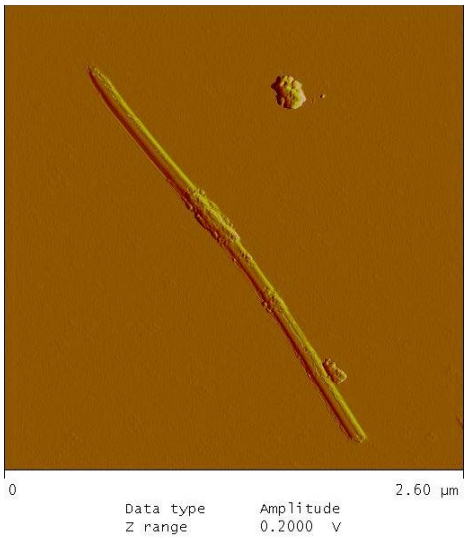

Figure 8. Micrograph obtained with AFM of purified SWNT sample.

In summary, small pellet sizes and low metal loadings at a Co/Mo ratio of 3 favor quality of the final product. The reduction has to be performed in-situ at intermediate temperatures, typically 500°C, in order to maintain a high quality and carbon yield. Intermediate reaction times also favor quality at the expense of yield, and the methane feed to the reactor has to be highly diluted in hydrogen in order to get selectivity

towards more crystalline forms of carbon/defect-free nanotubes. The surface area of the catalyst obtained by the combustion method plays a key role in the high carbon yields obtained. Large pellets of the catalyst, with less active surface area available to the reacting gases, significantly underperform compared to the fine powders in terms of carbon yield. Another evidence of this fact was provided by an alternative preparation method, in which the combustion step (made possible by the addition of citric acid as fuel) was eliminated, just finely grinding the mix of precursors and calcining it. Again, the results were poor in terms of carbon yield, showing how the combustion process is generating a fine powder with plenty of active area available for reaction. The intimate mixing that result upon combustion in Co/MgO preparations yields a very small amount of the active metal on the surface. In our case, Molybdenum helping stabilize the cobalt in fine particles on the catalyst surface, even in the calcined state. Molybdenum is acting in a synergistic way on this system. The composition of the reacting atmosphere also proved to have a significant influence on the quality of the materials being formed. While dilute methane atmospheres were necessary to ensure good activity and selectivity, the use of inert gases in high dilutions for the high metal loading catalysts can even change the product selectivity towards formation of double wall carbon nanotubes. The high-metal loading catalyst sample shows a split in the oxidation profile both under hydrogen and helium atmospheres, but the quality of the product is much better in the latter case. While we do not have a complete explanation for this behavior, it possibly has to do with the presence of larger clusters (since a higher amount of active metal has to be dispersed) and the absence of hydrogen attack. This is probably the main area where future research efforts in this area have to be focused in.

References

1. E. Flahaut, Ch. Laurent, A. Peigney, *Carbon* 43, 375 (2005).
2. J. Shen, M. Tu, C. Hu, *J. Solid State Chem.* 137, 295 (1998).

Project A.2) Tailoring (n,m) Structure of Single-Walled Carbon Nanotubes by Modifying Reaction Conditions and the Nature of the Support of CoMo Catalysts
PI: Daniel Resasco

One of the most attractive features of single-walled carbon nanotubes (SWNT) is that their electronic properties strongly depend on their diameter and orientation of the carbon hexagons that form their walls. These characteristics are uniquely specified by the chiral vector identified with the integers (*n*,*m*), but most synthesis methods result in a wide distribution of (*n*,*m*) species. In this project, the (*n*,*m*) population distribution of single-walled carbon nanotubes obtained on supported CoMo catalysts has been

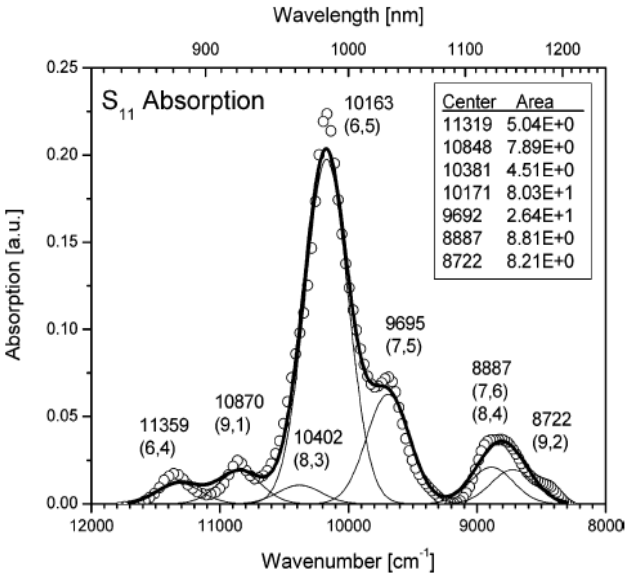

determined by photoluminescence and optical absorption.

It has been found that the (*n*,*m*) distribution can be controlled by varying the gaseous feed composition, the reaction temperature, and the type of catalyst support used. When using CO as a feed over $CoMo/SiO_2$ catalysts, increasing the synthesis temperature results in an increase in nanotube diameter, without a change in the chiral angle. The nanotube distribution shifts from a dominant (6,5) at the low-temperature end (700-750 °C, see spectrum above) to (7,6) and to (8,7) at 850°C. Interestingly, the nanotube diameter increases with temperature, but the chiral angle stays close to the armchair line. We have previously explained the increase in diameter with temperature in terms of a faster rate of metal agglomeration at higher temperatures that cause a shift to larger diameter caps during the nucleation that precedes the nanotube growth By contrast, by changing the support from SiO_2 to MgO, nanotubes with similar diameter but different chiral angles are obtained. Finally, keeping the same reaction conditions but varying the composition of the gaseous feed results in different (*n*,*m*) distribution. The clearly different distributions obtained when varying catalysts support and/or reaction conditions demonstrate that the (*n*,*m*) distribution is a result of differences in the growth kinetics, which in turn depends on the nanotube cap-metal cluster interaction.

Project A.3) Vertically oriented forests of SWNT.
PI: Daniel Resasco

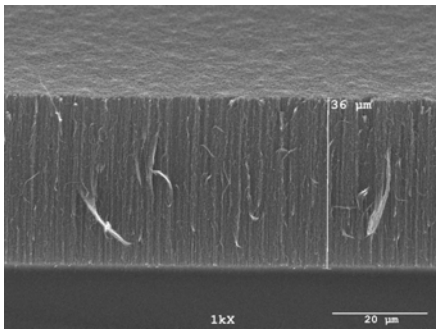

CO disproportionation on Co-Mo bimetallic catalysts has been used in the synthesis of vertically oriented forests of SWNT (see SEM image of forest). This is the first time that these forests are obtained by a CVD method at atmospheric pressure. Resonant Raman and transmission electron microscope (TEM) were employed to characterize the as-produced SWNT, which display a high purity and very low concentration of other carbon forms. Combination of AFM and SEM gives evidence for the crucial role of the surface distribution of the bimetallic (Co/Mo) catalyst particles on the substrate during the growth of SWNT.

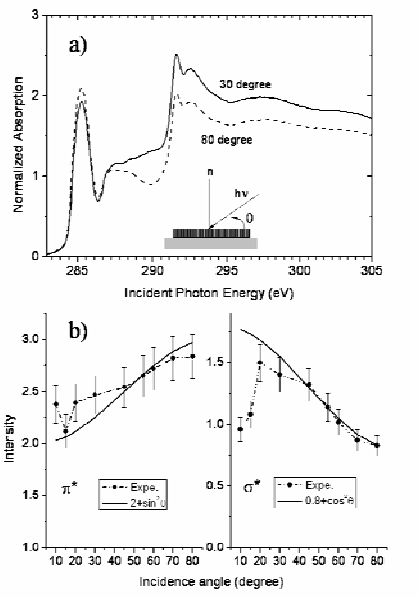

A detailed analysis of the structure of SWNT forests as a function of growth time reveals that a two-step process is responsible for the formation of a SWNT forest. The first step is the weaving of a crust of entangled SWNT which grow with different

rates and with random orientation over the surface. The second step is a concerted growth of vertically aligned SWNT constrained by the uniform top crust. Several techniques were employed to examine the growth process and the results are all consistent with this mechanism. The angle-resolved x-ray absorption near edge structure results (see Figure below) show that a fraction of the tubes on top of the forest are parallel to the surface, rather than perpendicular as the majority of the tubes in the forest. Direct SEM observations agree with this morphology. Several examples are presented to demonstrate that the crust influences the morphology of the resulting forest. Catalysts which are non-uniformly distributed on the substrate produce curved crusts instead of the consistent forest with a flat top obtained when the catalyst layer is uniform.

Project A.4) Controlling the growth of vertically oriented single-walled carbon nanotubes by varying the density of Co-Mo catalyst particles
PI: Daniel Resasco

A simple method to grow vertically aligned arrays of various forms of single-walled carbon nanotubes (V-SWNT) is reported. CO disproportionation on Co-Mo bimetallic catalysts has been used in the synthesis. Resonant Raman and transmission electron microscope (TEM) were employed to characterize the as-produced SWNTs, which display a high purity and very low concentration of other carbon forms. Combination of AFM and SEM gives evidence for the crucial role of the surface distribution of the bimetallic (Co/Mo) catalyst particles on the substrate during the growth of SWNT (see AFM and SEM images).

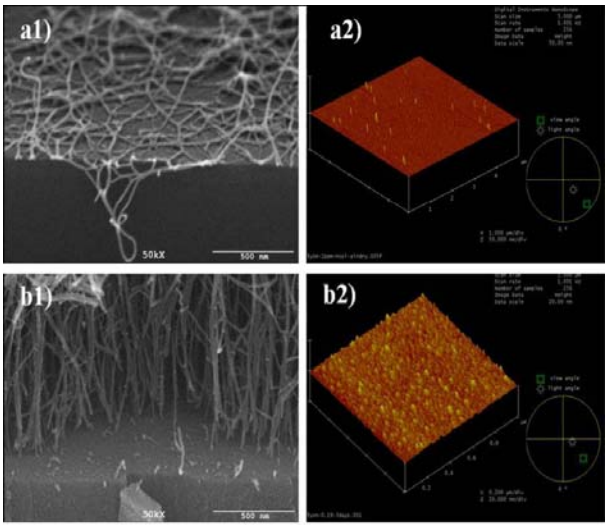

Project A.5) Nanostructured SWNT towers that exhibit superhydrophobic behavior.
PI: Daniel Resasco
We have discovered that while the contact angle for water-graphite is about 86°, that for SWNT-water greatly depend on the mesostructure of the nanotube system. That is, the same type of SWNT have very different wetting behavior depending on the nanotube arrangement. For example, the contact angle for a 2D mat of SWNT is close to that of graphite (86°); it goes up drastically to 135° for the nanotube forest, and become superhydrophobic (~180°) for a new type of SWNT arrangement that we call SWNT "towers."

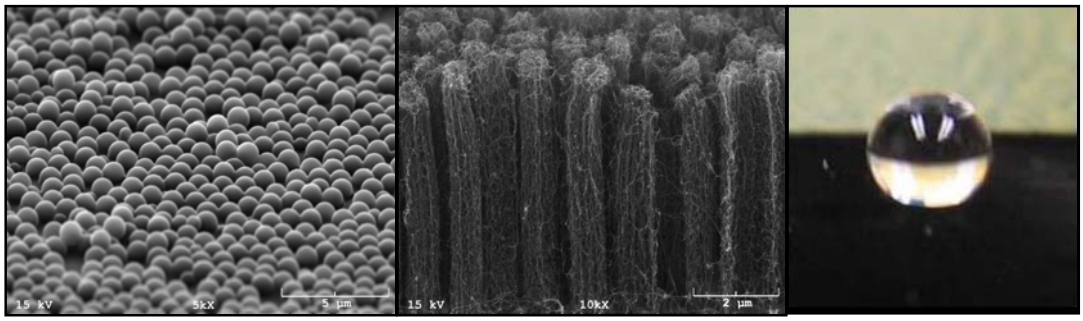

To achieve this SWNT array we have prepared the Co-Mo catalyst on silicon wafer employing the *nanosphere lithography method* that results in tailored distribution of catalysts and produces the distribution of SWNT shown in the image. These micro-towers of SWNT exhibit the "Lotus effect" that impart super-hydrophobicity to the surface.

Project A.6) Kinetic modeling of the SWNT growth
PI: Daniel Resasco
Steps considered in the model:
Specifically, the different stages considered in this model are the following:

a) Catalyst Activation:
This step takes into consideration the in-situ creation of the active sites that take place in the CoMoCAT process by the transformation of the CoMoOx precursor into the active species (i.e. reduced Co clusters) and will be modelled in terms of the conversion of oxidized sites (*Lox*) into active (reduced) sites (*Lred*). We define the new gas/solid interface as interface 1 (see schematic).

The balance of surface sites can be summarized as follows:

$$L_{ox} \xrightarrow{k_a} L_{red} \xleftrightarrow{k_d, k_r} L_{deact}$$

where Lox is the molar concentration of surface sites (mol ox. sites/g. cat) present on the catalyst before the introduction of CO, Lred is the concentration of reduced active sites, and Ldeact is the concentration of reduced but deactivated sites. It is assumed that the reduction step is irreversible, but the deactivation is reversible by the CO2 - C reaction. As mentioned above, only the reduced sites are active for the CO decomposition.

b) Decomposition of CO over the surface of the reduced Co cluster (interface 1) generating surface carbon species:
The surface fugacity of these carbon species is not simply in equilibrium with the gas phase CO, but rather is the result of the several phenomena that occur on the surface; they are i) the CO decomposition that generates surface C, ii) the C diffusion (both across the surface and into the metal particle), and iii) the reverse Boudouard reaction of C with gas phase CO2. The first one causes an increase in the carbon surface fugacity, the last two act as releasing paths for carbon and help keeping a fraction of the the surface clean.

c) Carbon diffusion, nucleation and growth of SWNT:
After the surface fugacity has reached a certain threshold, nucleation of ordered forms of carbon occur (e.g. hexagons. The formation of these nuclei generates a new interface between the catalyst surface and the nanotube (Lred/SWNT, interface 2 in the schematic). The carbon flux is maintained because the nanotube structure provides a thermodynamic sink for the carbon and as a result the carbon fugacity at the interface is kept low

.

d) Growth Termination:
Based on the concept of two interfaces one can envision two forms of nanotube growth termination. The first type of termination would occur at interface 1 by deactivation of the catalyst active sites, *Lred*. The second type would occur at interface 2 when the carbon concentration, CF, raises and approaches CS, thus eliminating the driving force for diffusion. As discussed below, the raising in CF may be due to a mechanical interference of the nanotube growth with its environment, which would hinder the free path of C through the catalyst-nanotube interface 2.

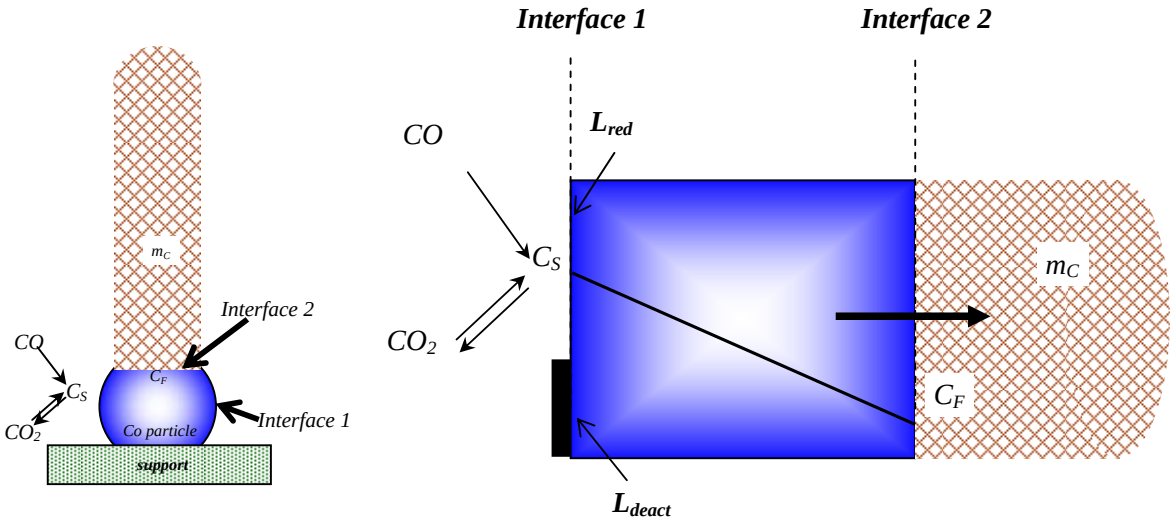

$$\psi_d = k_d\, p_{CO}^{m_d} \quad ; \quad k_d = k_{d_0} \exp(-E_d / RT)$$

$$\psi_r = k_r\, p_{CO_2}^{m_r} \quad ; \quad k_r = k_{r_0} \exp(-E_r / RT)$$

.

B) Carbon nanotubes for biomedical applications

PI: Roger G. Harrison

The goal of this research is to functionalize single-walled carbon nanotubes (SWNTs) with proteins and retain the protein's biological activity and also retain the near-infrared light absorbance of the SNWTs. An application identified for protein-

functionalized SWNTs is the treatment of cancer. The protein selected for study is human V, which has been found to bind selectively to the vasculature in tumors but not to the vasculature of normal tissue.

Prior research by the Resasco group and others has shown that covalent attachment of compounds directly to the SWNTs leads to the elimination of important features in the UV-vis-NIR absorption spectra. Therefore, we focused on physical adsorption of protein to the SWNTs. We first tested the model protein horseradish peroxidase (HRP), which is similar in size to annexin V. We used the sodium cholate suspension-dialysis method. In this method, the SWNTs are first suspended in an aqueous solution of the bile salt sodium cholate. The protein is then added, and the sodium cholate is removed using a dialysis membrane that allows it to pass through but not the protein. This resulted in a stable suspension of SWNTs, almost complete retention (98%) of the enzymatic activity of HRP, and the retention of a substantial fraction of the near-infrared absorption at 980 nm (**Figure 1**). To our knowledge, this is the first report of a protein being adsorbed on SWNTs with near complete retention of the activity of the protein. This work may find uses for numerous proteins in the biotechnology and medical fields. HRP itself is used in a number of detection methods for proteins, and the adsorption of HRP on SWNTs may find applications.

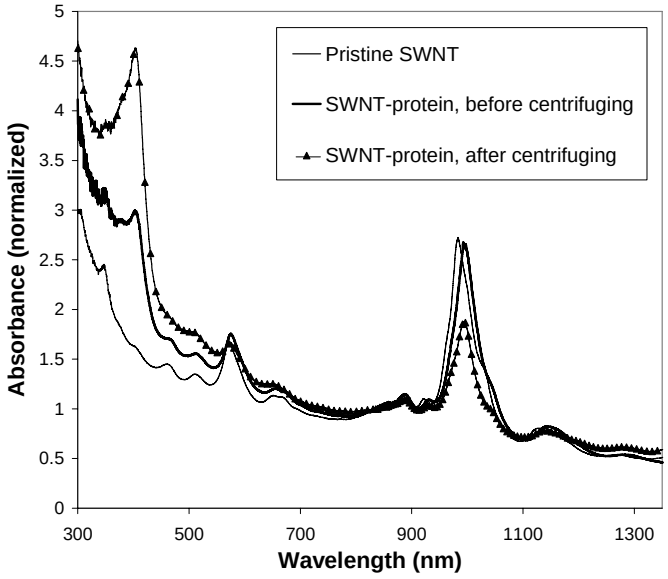

Figure 1. UV-vis-NIR absorption spectra of the pristine SWNTs suspended in sodium cholate, SWNT-protein complex before the final centrifugation, SWNT-protein complex after the final centrifugation.

When we used the sodium cholate suspension-dialysis method to adsorb annexin V on SWNTs, the SWNTs completely precipitated. Therefore, we developed a method to covalently attach annexin V to carboxymethylcellulose (CMC; 50 kDa) that had first been adsorbed on SWNTs to keep them in suspension. CMC had previously been used by the Resasco research group to suspend SWNTs. CMC has numerous carboxyl groups that can be linked to the amino groups in proteins. We used EDC (1-ethyl-3-[3-

dimethylaminopropyl] carbodiimide hydrochloride 1-ethyl-3) to link the carboxyl groups on CMC to the amino groups on both HRP and annexin V. For HRP, there was good retention of enzymatic activity (81% of the native activity) and a protein loading on the SWNTs of 3.0 mg protein/mg SWNTs. For annexin V, the protein loading was even higher—5.1 mg protein/mg SNWTs.

Work on this project was also directed to obtaining highly pure recombinant annexin V for use in various tests. The yield of purified protein was 59 mg per liter of cell culture. The purified protein was found to highly pure (>95% purity) and to be of the correct size by electrophoresis (**Figure 2**, lane 1). It was determined to have the correct amino-terminal sequence (first 6 amino acids). We have also found that the purified annexin V binds to phosphatidylserine (PS) immobilized on plastic microtiter plates. This binding is important since PS is exposed on the outside of the lining of the tumor vasculature but not for normal vasculature.

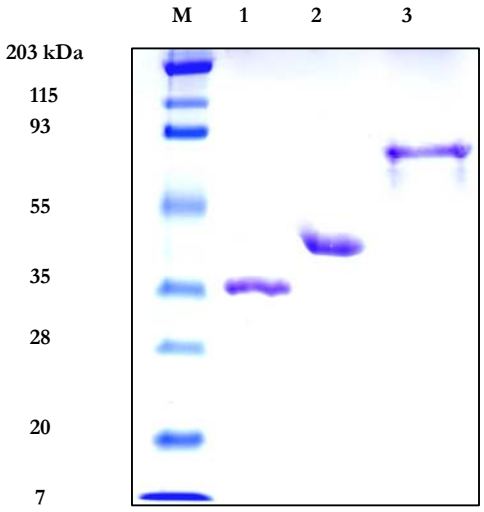

Figure 2. Electrophoresis analysis with Coomassie blue staining of purified annexin V (lane 1), L-methioninase (lane 2), and L-methioninase-annexin V fusion protein (lane 3; fusion protein consists of annexin V connected at its N terminus by a flexible linker to L-methioninase). These proteins were expressed by the vector pET-30 Ek/LIC in *E. coli* and then purified. M, marker proteins with molecular masses indicated on the left in kiloDaltons.

Carboxymethylcellulose (CMC; 30 kDa) was used to suspend SWNTs , and the unadsorbed CMC was removed by dialysis. We used EDC (1-ethyl-3-[3-dimethylaminopropyl] carbodiimide hydrochloride 1-ethyl-3) to link the carboxyl groups on CMC to the amino groups on annexin V. This gave a a suspension of SWNT-annexin V with a concentration of 163 mg protein per liter. Annexin V in the SWNT-annexin V complex was labeled with biotin. Human endothelial cells were grown as monolayers on 24-well plastic plates. The cells were exposed to a low level of hydrogen peroxide to expose phosphatidylserine (PS) on the surface of the cells and were then incubated with various concentrations of the SWNT-annexin V complex that had been labeled with biotin. After washing, the cells were incubated wth horseradish peroxidase (HRP)-streptavidin. (Streptavidin binds to biotin.) After washing, biotin-labeled annexin V was detected by the additon of substrate (*O*-phenylenediamine) that is converted by HRP to a product with a strong absorbance at 450 nm.

The results in Figure 3 show that the binding of SWNT-annexin V to human endothelial cells increased as its concentration increased. These results are consistent with those we have obtained previously for the binding of annexin V to PS immobilized on plastic microtiter plates. This data gives us a strong reason to believe that SWNT-annexin V injected into the bloodstream will selectively bind to the tumor vasculature, and therefore these bound SWNTs that are heated by near-infrared light will lead to death of the endothelial cells and subsequent cutoff of the blood supply to the tumor. The tumor will also be heated, which will cause tumor cells to die.

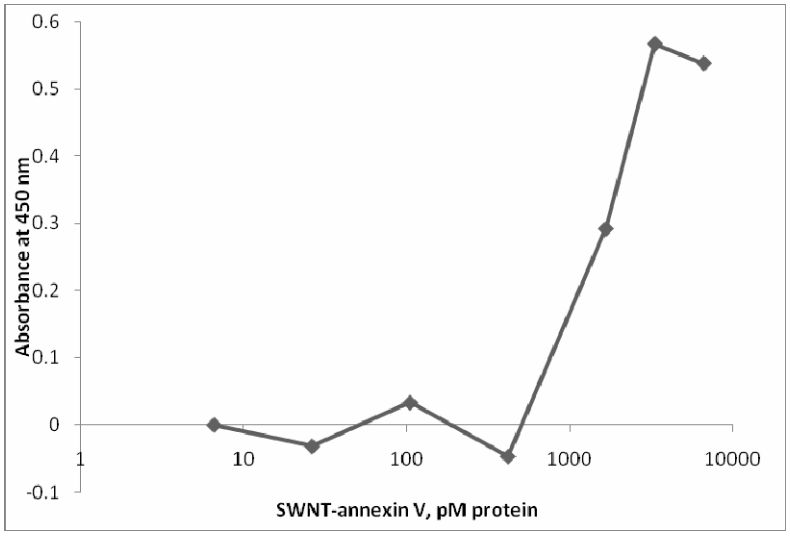

Figure 3. Binding of SWNT-annexin V (biotinylated) to human endothelial cells with exposure of PS induced by the addition of H_2O_2 (1 mM).

C) Simulation of Metal Nanoparticles supported on Single-Walled Carbon Nanotubes (SWNTs)

PI: Alberto Striolo

The financial support provided by the US Department of Energy through 'CANTEC I' has been instrumental for supporting one graduate student, Mr. Brian Morrow, since he joined the School of Chemical Biological and Materials Engineering in 2005. The continuation of the grant, 'CANTEC II', will allow Mr. Morrow to successfully complete the requirements for a Ph.D. in chemical engineering from the University of Oklahoma.

Within CANTEC I our group has explored the possibility of employing carbon nanotube (CNT) bundles as supports for heterogeneous catalysis. The catalytic sites we are interested in are metal nanoparticles (NPs) composed, in part or entirely of platinum atoms (Pt). The reason we are interested in such materials is their potential use in hydrogen or methanol fuel cells, as well as in other reactions relevant within the global search for alternative energy sources. Our hypothesis is that the topology of the solid support affects the morphology of the metal NPs, which, in turn, determines the NPs catalytic activity and selectivity. *Our goal is to quantify these effects*.

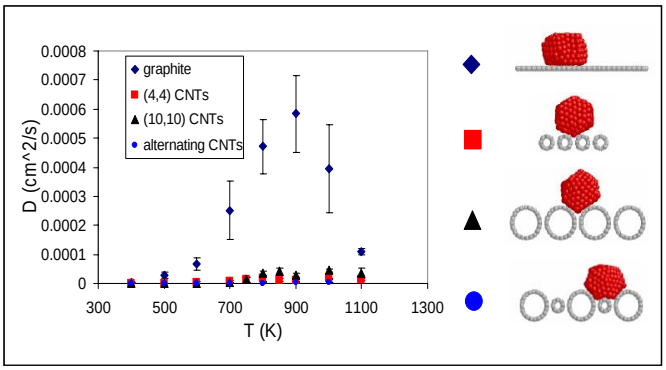

Fig. 1: Left: Diffusion coefficients for NPs of 249 Pt atoms on four substrates as a function of temperature. The reduced mobility of Pt nanoparticles on SWNTs suggests longer catalytic lifetime. Right: Simulation snapshots of the Pt NPs (red) on the substrates after 10 ns of MD simulations. Because the morphology depends on the substrate, reaction-specific catalysts can be designed.

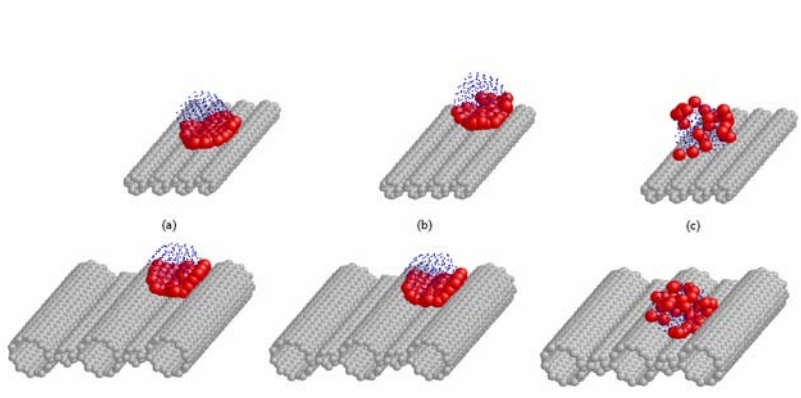

Fig. 2: 249 atom Pt cluster on (4,4) CNTs (top) and alternating CNTs (bottom). a) Initial configuration, b) after 7.5 ns at 600 K, c) after 7.5 ns at 1000 K. Pt atoms initially in contact with carbon atoms are red, all other Pt atoms are shrunk and blue. At 600 K (panel b), the metal atoms initially in contact with the substrate remain that way, suggesting gliding motion. At 1000 K (panel c), the Pt atoms initially in contact with the substrate are scattered throughout the NP, suggesting a disordered motion.

The morphology of supported Pt NPs depends on the diffusion of Pt atoms on the carbon nanotubes surface, a phenomenon related to the Ostwald ripening process. A detailed understanding of the Ostwald ripening mechanism will lead to more active and longer-lasting supported metal NPs. Further, it is not clear how the nanoparticles structure changes when they are supported on solid materials. Our results (**Fig. 1**) suggest that molecular dynamics (MD) simulations can answer these fundamental quests and guarantee progress in the field. Our simulations performed under the CANTEC I support were conducted for NPs deposited on four supports. The first is a rigid sheet of graphite; the second is composed by aligned (4,4) single-walled CNTs (SWNTs); the third by aligned (10,10) SWNTs; and the fourth by alternating (4,4) and (10,10) SWNTs. We found that the in-plane diffusion of the Pt NPs on graphite is at least one order of magnitude faster than that on SWNTs, suggesting that sintering of supported metal NPs is less likely on SWNTs. *This result promises longer expected lifetimes for the SWNT-based catalysts*. We also found that the structure of the supported NPs, i.e., the number of atoms with low coordination on the NPs surface, depends on the support

topography. *Thus we expect that the substrate greatly affects also the NPs catalytic properties*.

Further, our simulations allowed us to identify the diffusion mechanism for the metal NPs on the various carbon-based supports. We employed an autocorrelation function to determine whether the NPs glide or rotate as a rigid body on the solid supports and we found no evidence of NPs rotation (see **Fig. 2** for representative simulation snapshots). Our results indicate that a gliding motion occurs at T below the NPs melting T, and that a disordered motion takes place at larger T. These qualitative descriptions are corroborated by the results obtained for the autocorrelation function (not shown here for brevity, but these results can be found in our recent publication: J. Phys. Chem. C 111, 2007, 17905).

The results discussed above are encouraging because manipulating the solid support appears to be a viable route for controlling the catalytic activity of the supported metal NPs, thus allowing us to achieve 100% selectivity in catalysis, one of the grand challenges for the modern science of catalysis. In addition to controlling the crystallographic facets that enclose metal NPs, another possibility for manipulating the catalytic surface sites is to employ alloys.[1,2] We are currently conducting a series of MD simulations to test this possibility and to optimize our results by changing the relative composition of the metal NPs, as well as the T and the nature of the supporting materials. We expect at least one high-profile publication to result from these calculations (possibly one Nano Letter).

The work performed since the inception of CANTEC resulted in one published and one submitted peer-reviewed journal articles, two invited seminars, and three conference presentations:

D) Single-Walled Carbon Nanotubes in Polymers

PI: Brian P. Grady

Our primary accomplishment has been the development of a method to mix single-walled carbon nanotubes (SWNTs) in thermoplastic polymers that is easily scalable to an industrial scale.

There are four known ways to mix polymers with SWNTs and have reasonably good SWNT dispersion, i.e. significant debundling of the SWNTs. The first is to disperse the SWNTs in a solvent that is also a solvent for the polymer. This method works extremely well for water-soluble polymers, for example. However, if the desired application is something that is meant to be used as a solid, then it is extremely unlikely that a water-soluble polymer would be appropriate, since moisture from the air and/or environment would swell and/or dissolve the polymer. The second is to disperse the SWNTs in polymer monomer and then polymerize. For thermosetting polymers such as epoxies, such a method is entirely appropriate. However, for most thermoplastic polymers the large scale that such polymers are made at generally precludes this

---

[1] D. Bazin, C. Mottet, G. Treglia, New opportunities to understand heterogeneous catalysis processes on nanoscale bimetallic particles through synchrotron radiation and theoretical studies, Appl. Cat. A: General 200 (2000) 47.

[2] R. Imbhil, Model studies of catalysis with microstructured bimetallic surfaces, J. Mol. Catal. A: Chem. 158 (2000) 101.

method. The third is to disperse the SWNTs in a solvent that is also a solvent for the polymer. For most polymers, the appropriate solvents are significant health and fire hazards, and hence this method is not appropriate for most large scale applications, and is likely even not appropriate for small-scale applications.

The fourth method is to mix a water-dispersible polymer with SWNTs that have also been dispersed in water. There are no significant health or safety risks associated with this method, and the nanotube content in the polymer can be easily controlled via the volume of water used in the mixing step. Acrylic latex paints are the most common water dispersible polymers widely available, but other types of polymers such as polyurethanes, polyamides, polyesters etc. are also commercially available. As should be clear, there is a significant environmental driving force to develop water-dispersible polymers so as to eliminate the use of volatile organic compounds. Hence, the number of water-dispersible polymers available commercially is only expected to grow. Our group has spent significant effort into developing this method of dispersing SWNTs.

Our group was not the first to mix latex with dispersed single-walled carbon nanotubes; , however, the amount of material characterization our group did with these materials was significantly more than done previously. Specifically, we characterized the materials for a full-range of electrical, mechanical, solid-state rheological, and thermal (both heat capacity and thermal conductivity) properties. The percolation threshold was 0.2%, which indicates that SWNT dispersion was good. There was an increase in tensile strength and modulus, although at fractions greater than 1% by tubes the increases were not very large. The following summarizes unique observations, i.e. observations that as far as we are aware have not been reported in the literature for any previous SWNT-polymer composite.

a) The glass transition temperature (Tg) of a SWNT-polymer composite increases slightly with increasing SWNT content or shows no change; clearly the effect is not large. A reduction in heat capacity jump at the glass transition, attributed to the formation of a rigid amorphous fraction, has been seen for the first time in SWNT-polymer composites. Others have likely not reported this effect because high volume fractions (>5% NT) are necessary to be sure that the decrease is not simply data scatter.

b) Although the thermal conductivity of SWNTs is extremely high, the thermal conductivity of SWNT-polymer composites is orders-of-magnitude less than a simple mixing rule would predict. It is well-known from theoretical studies as well as experimental studies on other materials that the reason for this is the modulus mismatch between the SWNT and polymer, i.e. the Kapitza resistance. Our group was able to show that the thermal conductivity decreased as a SWNT-polymer composite went from a glass to a melt; i.e. as the modulus mismatch grew, the thermal conductivity dropped. Although we certainly did not doubt the theory, this experiment does represent the first time to our knowledge that the Kaptiza resistance was confirmed experimentally in SWNT-polymer composites.

c) It is well-known that the introduction of SWNTs into a polymer causes the formation of a network-like structure consisting of nanotube/polymer entanglements, which is typically measured as a flat G' at low frequency in oscillatory shear measurements. Our group was able to show that the same phenomena can be measured in tension rather than in shear; which has the advantage of determining the temperature dependence of the network structure in a much simpler fashion. A tensile method also confirms that the network effect will be found in the elongational viscosity as well, at least at low elongation rates.

E) Biosensors from Single-Walled Carbon Nanotubes

PI: David Schmidtke

Layer-by-layer glucose sensors based on SWNTs

Nanoscaled multilayered films sensitive for glucose were fabricated by the electrostatic layer-by-layer (LBL) assembly of a positively charged redox polymer, poly[(vinylpyridine)Os(bipyridyl)$_2$Cl$^{2+/3+}$] (PVP-Os), and a negatively charged enzyme, glucose oxidase (GOX), or a GOX solution containing single-walled carbon nanotubes (SWNTs) on gold electrodes. The self-assembly buildup of multilayer films was followed by UV-vis spectroscopy, ellipsometry, and cyclic voltammetry, while XPS measurements provided evidence of enzyme adsorption onto SWNTs. By varying the number of bilayers (PVP-Os/GOX) not only was the thickness of the films controlled (thickness = 2 – 30 nm), but both the electrochemical and enzymatic responses of the sensors could be controlled as well. Incorporation of SWNTs into the LBL films did not appear to affect the redox potential of the films (300 mV) or the reversibility of electron transfer (ΔEp = 35 mV). However, incorporation of SWNTs into structures with more than one bilayer did result in a 2-4-fold increase in the electrochemical response, while the enzymatic response to response to glucose was increased 6-17-fold. The increased current densities (90 μA/cm^2) exhibited by the films which had SWNTs incorporated in them and the fact that the LBL technique is independent of electrode topology and size make them attractive materials as nanoscale building blocks for a number of novel applications such as glucose sensing, immunosensors, and DNA sensors. These results have been published in the journal Langmuir

GOX adsorption onto SWNTs

We have developed a procedure to adsorb glucose oxidase (GOX) onto single-walled carbon nanotubes using a sodium cholate suspension-dialysis method. This procedure is based on the method developed by Dr. Resasco and Dr. Harrison to adsorb horseradish peroxidase onto SWNTs. This method allows for the biological activity of GOX to be retained upon adsorption and results in a stable SWNT suspension. We are currently utilizing these GOX coated SWNTs to develop novel nanoscaled biosensors and to investigate the role of individual nanotubes vs nanotube bundles in enzymatic electrooxidation of GOX in redox polymer films.

Lactate Oxidase Biosensors

We are developing sensors for lactate by incorporating SWNTs into redox polymer films of PVP-Os containing lactate oxidase. Initial results suggest that the presence of SWNTs in the films results in a 2-fold increase in the sensor's response to lactate, and that the SWNTs must be mixed with the redox polymer first prior to addition of the enzyme and crosslinker. We are currently in the process of writing a manuscript on these results.

F) Production of Aluminum/CNT Composites using Aqueous Dispersion

PI: Brandon Olson

The extraordinary properties of Carbon NanoTubes (CNT) make them an excellent candidate for use in composite materials, yet dispersion of the nanotubes within the matrix material has proven to be a formidable obstacle in their development. This is especially true of metal-matrix composites due to the general incompatibility of standard nanotube debundling techniques and the processes used in metal production. Previously supported work has successfully identified a preparation technique whereby nanotubes can be distributed throughout the matrix metal without compromising its integrity.

Collaborative effort within the CaNTeC group has yielded a truly unique composite preparation approach that combines aqueous surfactant dispersion with powdered metal sintering. Specialized surfactants are first used to debundle and disperse the carbon nanotubes in an aqueous suspension (Fig. 1); following which, the powdered matrix metal is mixed into suspension with the nanotubes. The suspension is then filtered and dried leaving debundled carbon nanotubes diffusely mixed within the metal matrix powder. The composite mixture is then mechanically pressed and sintered (Fig. 2) Because sintering temperatures are typically held below (80-95%) the matrix melting point, the mobility of the nanotubes remains sufficiently low to maintain a homogenous dispersion throughout the composite. Preliminary experiments have shown this technique to be effective in dispersing nanotubes at weight loadings of approximately 0.2% without degrading the matrix mechanical properties.

Initially, there existed considerable uncertainty how powdered matrix metal would respond to aqueous suspension and surfactant treatment. Thus, a significant effort was directed at identifying which of the myriad of available surfactants would simultaneously disperse the CNT's without inhibiting the sintering process or the integrity of the aluminum particles.

Preliminary estimates indicated that a lithium-based dispersion process, commonly used in CNT processing, appeared to have properties favorable for integration with powdered metal. A 20% excess solution was used to disperse single wall nanotubes (0.1% by weight) as well as powdered Al (D_{ave}=0.5-0.8μm). After drying and compaction, the composite was sintered at 20^{o}C less than the matrix melting temperature. Post sintering examination showed that the SWNT *were* effectively dispersed, yet the surfactant treatment tended to make the samples very brittle (Fig. 3).

While the preliminary success in dispersing the SWNT was promising, the failure in matrix degradation indicated that the type of surfactant employed would have a critical effect on the overall properties of the composite. Morphological examination showed that the dispersing agent was simply carbonizing during the sintering process, leaving a large amount of amorphous material in the matrix. This suggested that a surfactant capable of completely dissociating at high temperatures would be advantageous.

A search of alternative formulations identified Triton X100 as a surfactant that would dissociate into gaseous components at moderate temperatures, thus allowing vacuum removal. Low concentrations of this surfactant have also been shown to effectively disperse single and multiwall nanotubes. A series of samples were prepared and

sintered with the following compositions: 1) neat Al, 2) Triton/Al, and 3) CNT/Triton/Al at a CNT weight loading of 0.1%. The Triton surfactant was mixed at 20% excess.

During subsequent mechanical testing it was determined that the neat Al and Triton/Al samples displayed essentially identical stiffness and tensile strength. Thus, it can be concluded that the surfactant treatment had no adverse impact on the mechanical properties of the aluminum matrix. The CNT/Triton/Al sample displayed slightly elevated (~5%) tensile strength; a result that would appear to be consistent with its low weight loading. Morphological SEM examination indicated that the nanotubes appeared to be *well dispersed* throughout the Al matrix before and after sintering (Fig. 4). The results of these preliminary experiments can be summarized as follows:

1) The Triton X100 surfactant effectively debundled and dispersed the suspended nanotubes without degrading the properties of the matrix metal or the sintering quality.
2) In range of temperatures examined, there was *no* strong correlation between mechanical properties (stiffness and yield strength) and sintering temperature.
3) Extremely small powder diameters (<1μm) tend to degrade the properties of the sintered metal. It is theorized that the increased amount of oxidized surface inhibits sintering.